Development of a Human-Body Dynamic Model for Paraplegics Wearing an Ambulatory Exoskeleton

F. Firmani[1], E. J. Park[2]

[1] *Department of Mechanical Engineering, University of Victoria, ffirmani@me.uvic.ca*

[2] *School of Engineering Science, Simon Fraser University, ed_park@sfu.ca*

Abstract

Kinematic and dynamic models of a human body are presented. The models intend to represent paraplegics wearing an ambulatory exoskeleton. The proposed exoskeleton controls completely the motion of the hip and knee joints, i.e., each lower extremity contains four actuators, three at the hip joint and one at the knee joint. A spring-loaded ankle-foot orthosis completes the exoskeleton. The kinematic model involves a large number of degrees of freedom, 34-dof. The dynamic model presents a general formulation that can be implemented for any human task – walking, running, jumping, climbing stairs, etc. Traditional dynamic models simplify the motion of bipeds by considering a limited number of movements contained in the sagittal plane and by focusing on a particular task. A 3D model of a human body has been developed to simulate motion.

Keywords: exoskeleton, biomechanics, dynamics, kinematics

Développement d'un Modèle Dynamique du Corps Humain pour des Paraplégiques qui Portant un Exosquelette Ambulatoire

Résumé

Des modèles cinématiques et dynamiques d'un corps humain sont présentés. Les modèles cherchent à représenter des paraplégiques qui portent un exosquelette ambulatoire. L'exosquelette proposé commande complètement le mouvement des articulations dans les hanches et les genoux, i.e., chaque extrémité inférieure contient quatre actionneurs, trois dans la jointure de la hanche et un dans la jointure du genou. Une orthèse avec des ressorts chargés dans la cheville et le pied complète l'exosquelette. Le modèle cinématique contient un grand nombre de degrés de liberté, 34-dof. Le modèle dynamique présente une formulation générale qui peut être employé pour n'importe quelle tâche humaine – marcher, courir, sauter, monter les escaliers, etc. Les modèles dynamiques traditionnels simplifient les mouvements des bipèdes en considérant un nombre limité de mouvements contenus dans le plan sagittal et ils se spécialisent dans une tâche particulière. Un modèle 3D d'un corps humain a été développé pour simuler le mouvement.

Mots-clé: exosquelette, biomécanique, dynamique, cinématique

1 INTRODUCTION

Exoskeletons are wearable devices that mould around the human body. An exoskeleton is composed of links and joints that match externally those of the person who wears it. Lower limb exoskeletons can be used for different purposes – performance amplification, locomotion (ambulatory), and rehabilitation. In general, joint actuation and sensing depends on the type of application.

Perfomance Amplification. The purpose of this type of exoskeleton is to increase strength and endurance of the user. Military has been appealed by the idea of developing an exoskeleton to assist infantry soldiers. In 1968, General Electric envisioned Hardiman [1], a combination of upper and lower exoskeletons. BLEEX [2] and XOS [3] are modern prototypes of infantry-soldier exoskeletons that are powered with portable internal combustion engines. HAL-5 [4], a full-body battery-powered suit, was designed to aid elderly and disable people. For power amplification exoskeletons, the objective is to assist the joints that require the greater torques, i.e., the joints whose axes are normal to the sagittal plane. A main challenge is to detect the motion intention of the user. This is accomplished by measuring brain signals that flow along muscle fibbers, these signals are generally sensed with electromyograms (EMGs). Then, a control unit determines the required assistive power and commands the actuators to produce a specific torque.

Ambulatory. In the late 60's, Vucobratović *et al.* [5] at the Mihailo Pupin Institute developed the first legged locomotion system to assist patients walk by commanding the exoskeleton to move pre-defined trajectories. Patients with diverse degrees of paralysis tested the device with the aid of crutches. The success of the project was affected by the limited technology at the time; nevertheless, the presented theoretical results still remain a reliable principle for the dynamic control of biped robots. A contemporary work was carried out at the University of Wisconsin [6]. The design involved rotary hydraulic actuators at the hip and knee joints. The patient required the use of canes for balancing. Both of these pioneering exoskeletons were controlled by computers that were not mounted on the device. To date only a few ambulatory exoskeletons have been built. An ambulatory system that combines a powered exoskeleton with a customized walker was designed at Sogang University [7]. The walker ensures complete balance and reduces the weight of the device by housing the battery, dc motors, and control unit. Cables transmit power to the joints. ReWalk developed by Argo Medical Technologies Ltd. enables paralysed people, with the aid of crutches for balance, to stand up, sit down, walk about including slopes, and even climb stairs [8]. ReWalk features servomotors located at the hip and knee joints, rechargeable batteries, and a wrist remote control that dictates the type of desired motion. Since ambulatory exoskeletons are meant to be used by paraplegics and people with severely impaired locomotion capabilities, two crucial problems must be considered – ensuring full balance and determining the intention of motion. To overcome these problems, external devices have been considered – crutches, canes, or walkers are used to ensured balance, whereas joysticks or keypads are used to dictate the desired motion.

Rehabilitation. Exoskeletons for rehabilitation provide joint trajectories of the gait cycle and a uniform stiff during the cycle. Colombo *et al.* [9] developed a size-adjustable driven gait orthosis. The knee and hip joints are actuated; whereas the ankle joint is controlled with a passive foot lifter. The LOwer-extremity Powered ExoSkeleton (LOPES) provides gait rehabilitation on treadmills [10]. The mechanical hip joint allows two rotations. A research team at the University of Michigan developed a knee-ankle-foot orthosis, which is powered with artificial pneumatic muscles [11].

In recent years, advancements in sensor, actuator, and microprocessor technology could bring about potential ambulatory exoskeletons that need not require the use of external devices. Developments in the above-mentioned applications can be merged to attain this concept of autonomous exoskeletons. The purpose of this work is to build a platform in which potential control strategies and sensor arrangements can be tested. For control, the goal is to have an accurate dynamic model which would ensure the balance of the user, but at the same time be efficient, as this formulation must be processed real time. For sensing, this platform can be used as a metric to test the accuracy of the readings. This would establish the roots for the development of an autonomous exoskeleton.

2 KINEMATICS

The human skeletal system is extremely complex. Zatsiorsky [12] estimates that there are 148 movable bones and 147 joints in the human body, which represents 244 degrees of freedom (dof). Herein, the most significant human body segments and joints will be considered. The proposed model contains 34 dof, which are summarized as follows – torso (3-dof), neck (3-dof), legs (2×7-dof), and arms (2×7-dof).

Trunk and Neck. A kinematic model of the human torso is extremely difficult to reproduce. The spine contains 24 mobile segments that are divided into four regions – cervical, thoracic, lumbar, and sacrum. The motion of the vertebrae, which can rotate and translate, are coupled. The spine as a whole can produce only three movements flexion-extension, lateral flexion, and axial rotation [12]. Commonly, the first 30 degrees of flexion occur in the lumbar region (lumbar-pelvic rhythm) and then the pelvis tilts. Lateral and axial rotation occurs in the thoracic and lumbar regions to various degrees. To maintain the kinematic model as simple as possible, only the rotations at the lumbar region (sacroiliac joint) are considered. The cervical spine consists of eight joints of complex geometry. The movement of the neck can be described through arcs given by the coupled cervical vertebrae. To reduce the complexity of the model, the proposed kinematic model involves a ball-and-socket joint located at the boundaries of the cervical and thoracic regions.

Lower Limbs. The hip joint is a ball-and-socket joint that connects the pelvis with the femur. The hip joint allows three rotational motions known as flexion/extension (forward/backward leg swing), abduction/adduction (outward/inward lateral leg swing), and medial/lateral rotation (internal/external rotation about the longitudinal axis of the femur). The knee joint connects the femur, patella, tibia, and fibula bones. A knee joint represents a condylar joint which allows a primary motion about one axis (flexion/extension) and a small amount of movement about another axis (medial/lateral rotation). Feet is one of the most complex orthopedic structures of the human body. The ankle and foot contain 33 joints and is divided into three parts – hindfoot, midfoot, and forefoot [13]. In this work, the biomechanic analysis of the foot is limited to the hindfoot and the metatarsophalangeal (MTP) joints. The hindfoot is comprised of the calcaneus (heel), talus, navicular, and cuboid bones. Three degrees of freedom of motion are achieved through the connections of these bones. The ankle joint is a hinge joint that connects the tibia and fibula with the talus bone. The motion is denoted as dorsiflexion when toes go up and plantar flexion when toes down. The subtalar joint connects the talus and the calcaneus (heel) bones allowing inversion when one walks on the side of the foot and eversion, its opposite. The transverse tarsal joint hinges the talus and calcaneus bones with the navicular and cuboid bones. The transverse tarsal joint permits adduction

(toe-in) and abduction (toe-out) movements which are needed as shock absorbent during the heel strike phase while walking. The MTP joints connects the metatarsal bones with the phalanges. These joints help to stabilize the foot and assist in the push-off stage during gait. Excluding the other joints of the mid and forefoot, there are nine independent joints in a human lower limb. From these joints, the medial/lateral rotation of the knee joint, which serves to relax the tension in the collateral ligaments to allow flexion, and the transverse tarsal joint, which functions as a shock absorbent, will not be considered. The range of displacement of these joints is very small compared to the rest of the joint displacements. Thus, this yields seven dof to be modelled.

Upper Limbs. The shoulder is a ball-and-socket joint that connects the humerus of the upper arm with the clavicle (collarbone) and the scapula (shoulder blade). The elbow is a hinge joint (flexion/extension) that connects the humerus with the radius and ulna bones of the forearm. The rotation of the forearm (pronation) occurs at the radioulnar joint. The wrist joint connects the radius and ulna with the proximal part of the carpal bones allowing rotation about two axes – flexion/extension and abduction/adduction. It is worth of mentioning that circumduction of the wrist, which allows a conical rotation of the hand, is the combination of the above-mantioned two rotations and not an independent motion. Thus, each upper limb is modelled with seven dof.

Kinematic Model. The pelvis segment was considered the rigid body that defines the location and orientation of the human body with respect to an inertial reference frame. Let $\mathbf{P} = [P_{x_{iL}},\ P_{y_{iL}},\ P_{z_{iL}}]$, where i denotes either left (L) or right (R), be the position vector of from the pelvis centre of mass (Pv) to the hip joint. Similarly, vector $\mathbf{P} = [P_{x_{iA}},\ P_{y_{iA}},\ P_{z_{iA}}]$, denotes the position of the shoulders with respect to the torso centre of mass (T). The Denavit and Hartenberg parameters of the lower and upper limbs are shown in Table 1. Shown in Figure 1 is the proposed kinematic model of the human body. Note that the the joint that represents the medial/lateral rotation (or rotation about the longitudinal axis of the femur) provides the same kinematic motion as if it was at the hip. The angle β represents the q angle of the knee, i.e., the angle between the femur and tibia bones. The angle γ provides the inclination of the foot, which represents the difference in elevation between the ankle and MPT joints.

Human-Body 3D Model. A human-body 3D model[3] has been adapted to have a more realistic representation of the system. Each segment of the model is a rigid body that is graphically represented by surfaces. These surfaces are generated by enclosing points with polygons. The location of the points were modified so that the proximal joint centre[4] of a segment is located at the origin of an inertial reference frame and the segment is aligned along the x or z axis depending on the definition of the segment, i.e., link length or link offset. The human body is formed based on the Denavit and Hartenberg parameters. The location and orientation of a segment in space is defined by a homogeneous transform matrix. By doing this, motion of the segments can be achieved by manipulating the joint angles. To improve the animation, the segments were converted into objects in Matlab, and with the aid of handle graphics the new location and orientation of the segment in space can be efficiently regenerated. Figure 2, shows the human-body model in its zero-displacement configuration posture.

[3]The human-body model is based on a Matlab open source program created by Tordoff and Mayol [14]. The file consists of a collection of body segments and polygons that were originally created in VRML by Cindy Ballreich.

[4]The proximal joint is referred to as the joint that is closer to the pelvis along the chain of links.

Table 1: Denavit and Hartenberg Parameters of Lower and Upper Limbs

	Left Leg				Right Leg				
i-1	α_{i-1}	a_{i-1}	d_i	θ_i	α_{i-1}	a_{i-1}	d_i	θ_i	*i*
Pv	*0*	$P_{x_{LL}}$	$P_{z_{LL}}$	*0*	*0*	$P_{x_{RL}}$	$P_{z_{RL}}$	*0*	*0*
0	*-90*	*0*	$P_{y_{LL}}$	$\theta_1 + 90$	*90*	*0*	$P_{y_{RL}}$	$\theta_1 - 90$	*1*
1	*90*	*0*	*0*	$\theta_2 - 90 - \beta$	*-90*	*0*	*0*	$\theta_2 + 90 + \beta$	*2*
2	*-90*	*0*	d_3	$\theta_3 - 90$	*90*	*0*	d_3	$\theta_3 + 90$	*3*
3	*90+β*	*0*	*0*	$\theta_4 + 90$	*-90-beta*	*0*	*0*	$\theta_4 - 90$	*4*
4	*0*	l_4	*0*	$\theta_5 + \gamma$	*0*	l_4	*0*	$\theta_5 - \gamma$	*5*
5	*90*	*0*	d_6	θ_6	*-90*	*0*	d_6	θ_6	*6*
6	*-90*	*0*	*0*	$\theta_7 - 90 - \gamma$	*90*	*0*	*0*	$\theta_7 + 90 + \gamma$	*7*
7	*0*	L_7	*0*	*0*	*0*	L_7	*0*	*0*	*toe*

	Left Arm				Right Arm				
i-1	α_{i-1}	a_{i-1}	d_i	θ_i	α_{i-1}	a_{i-1}	d_i	θ_i	*i*
T	*0*	$P_{x_{LA}}$	$P_{z_{LA}}$	*0*	*0*	$P_{x_{RA}}$	$P_{z_{RA}}$	*0*	*0*
0	*-90*	*0*	$P_{y_{LA}}$	$\theta_1 + 90$	*90*	*0*	$P_{y_{RA}}$	$\theta_1 - 90$	*1*
1	*90*	*0*	*0*	$\theta_2 - 90$	*-90*	*0*	*0*	$\theta_2 + 90$	*2*
2	*-90*	*0*	d_3	$\theta_3 - 90$	*90*	*0*	d_3	$\theta_3 + 90$	*3*
3	*90*	*0*	*0*	θ_4	*-90*	*0*	*0*	θ_4	*4*
4	*-90*	*0*	d_5	θ_5	*90*	*0*	d_5	θ_5	*5*
5	*90*	*0*	*0*	$\theta_6 + 90$	*-90*	*0*	*0*	$\theta_6 - 90$	*6*
6	*90*	*0*	*0*	θ_7	*-90*	*0*	*0*	θ_7	*7*
7	*0*	L_7	*0*	*0*	*0*	L_7	*0*	*0*	*fing*

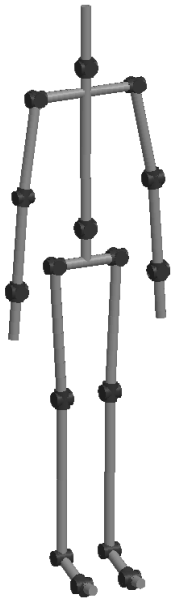

Figure 1: Joint Layout of Human Body

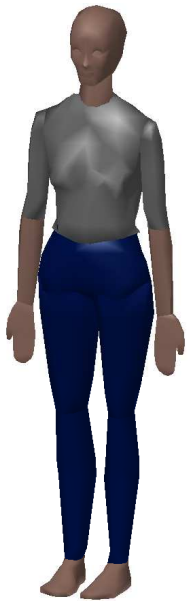

Figure 2: 3D Human-Body Model

3 DYNAMICS

3.1 Anthropometric Parameters

The dynamic model of the human body requires a fair estimation of measurements – mass, location of centre of mass, and radii of gyration or moments of inertia – of each body segment. Different techniques have been proposed to determine the magnitude of these parameters. There is a wide discrepancy among the results published in the literature, in part due to the choice of segment boundaries, particular dimensions of the tested individual(s), and the technique employed. Early works dealt with cadavers [15] and geometric modelling [16]. Modern technology has allowed researchers to perform in vivo measurements using medical diagnostic devices such as gamma ray scanners, computed tomography, and magnetic resonance imaging. Herein, the results obtained by Zatsiorsky *et al.* [17] and later adjusted by De Leva [18] will be employed. Zatsiorsky *et al.* determined with a gamma-ray scanner the relative body segment masses, location of the centres of mass, and radii of gyration of 100 male and 15 female individuals. De Leva adjusted these values as the originals were distant from the joint centres that are conventionally used.

For this work the lengths of segments in Figure 2 are used. The total hight of the human body is 1.70m and the weight was considered at 63kg. De Leva reported the centre of mass location and radii of gyration as a percentage of the longitudinal length of each segment. The only modification made was that De Leva considered three parts of the torso; whereas in this work thorax and abdomen were assumed as one segment. Parallel axis theorem was used to combine the inertia properties of these two parts. The anthropomorphic parameters are presented in Table 2.

Table 2: Anthropomorphic Parameters

Segment	Mass (kg)	Longitudinal Length (m)	Centre of Mass (proximal) (m)	Radii of Gyration (m)			Moments of Inertia (kgm^2)		
				r_s	r_t	r_l	I_{xx}	I_{yy}	I_{zz})
Skull	4.208	0.2050	0.1847	0.0677	0.0736	0.0652	0.0193	0.0228	0.0179
Torso	26.819	0.5325	0.3115	0.1901	0.1805	0.0911	0.9692	0.8739	0.2224
Thrx/Abd	18.963	0.3525	0.2212	0.1440	0.1272	0.0956	0.3933	0.3067	0.1734
Pelvis	7.856	0.1800	0.0886	0.0779	0.0724	0.0799	0.0477	0.0411	0.0502
Thigh	9.311	0.3616	0.1304	0.1334	0.1316	0.0586	0.1658	0.1613	0.0320
Shank	3.030	0.4337	0.1915	0.1175	0.1158	0.0403	0.0419	0.0406	0.0049
Foot	0.813	0.2524	0.0989	0.0755	0.0704	0.0351	0.0046	0.0040	0.0010
Upper Arm	1.607	0.2649	0.1496	0.0736	0.0689	0.0392	0.0087	0.0076	0.0025
Forearm	0.869	0.2556	0.1163	0.0667	0.0657	0.0240	0.0039	0.0038	0.0005
Hand	0.353	0.1780	0.0765	0.0945	0.0808	0.0596	0.0032	0.0023	0.0013

3.2 Dynamic Model

Dynamic models of the human body are commonly very simple with only a limited number of movements contained in the sagittal plane. The implementation of these dynamic models in powered exoskeletons are valid for those cases in which balance can be ensured by the user; for example, exoskeletons used by healthy people or combined with the aid of external devices, such as

crutches, canes, or walkers. As a preliminary picture of the exoskeleton, there will be two mechanical devices. The first mechanism is a hip-knee powered orthosis which provides motion to the user. To ensure complete balance and mobility, all the degrees of freedom will be controlled. The second device is a spring-loaded ankle-foot orthosis that provides enough support to the human body joints by adapting its mechanical configuration depending on the action taken by the user.

The dynamic analysis of robotic systems is composed of two parts – forward and inverse dynamics. In forward dynamics, the interest is to determine the motion of the system as an effect of the applied torques or forces. This formulation is employed to *simulate* the motion of the system as a response to forces. The inverse dynamics, on the other hand, determines the torques or forces that are required to provide a desired motion. The desired motion is generally established with a trajectory generator. The inverse dynamic formulation is employed to *control* the system by tracking the desired motion, as errors exist due to the imperfection of the dynamic model and the inevitable presence of disturbances.

The proposed dynamic model resembles the one presented by Vukobratović *et al.* [19]. The fundamental concept of the dynamic model is to represent the human body as a free spatial system (flier) that interacts with the exterior through contact forces. The nature of the model is based on the biomechanical principals of the human body. A free spatial system is composed of a main body (pelvis) and multiple branches attached to it. In order to formulate the dynamic equation, the state variables must be identified – pelvis description variables and exoskeleton actuated joint variables. The pelvis requires six coordinates to be described in space $\mathbf{x}_{\boldsymbol{T}} = [x,\ y,\ z,\ \phi,\ \varphi,\ \psi]^{\mathsf{T}}$, where x, y, and z represent the location of the centre of mass; whereas, ϕ, φ, and ψ represent the Euler angles (roll, pitch, and yaw, respectively). The joint displacements of the actuated joints are denoted as $\boldsymbol{\theta_k} = [\theta_{k_1},\ \theta_{k_2},\ ...,\ \theta_{k_n}]^{\mathsf{T}}$, where *k* denotes the leg (left or right) and n denotes the number of actuated joints per leg, $n = 4$. Therefore, the following state variable vector results

$$\boldsymbol{\Theta} = [x, y, z, \phi, \varphi, \psi, \theta_{1_1}, \theta_{1_2}, \theta_{1_3}, \theta_{1_4}, \theta_{2_1}, \theta_{2_2}, \theta_{2_3}, \theta_{2_4}]^{\mathsf{T}}. \tag{1}$$

The general equation of a dynamic spatial system is given by the following formulation,

$$\mathbf{M}(\boldsymbol{\Theta})\ddot{\boldsymbol{\Theta}} + \mathbf{V}(\dot{\boldsymbol{\Theta}}, \boldsymbol{\Theta}) + \mathbf{G}(\boldsymbol{\Theta}) = \mathbf{Q} \tag{2}$$

where $\mathbf{M}(\boldsymbol{\Theta})$, $\mathbf{V}(\dot{\boldsymbol{\Theta}}, \boldsymbol{\Theta})$, $\mathbf{G}(\boldsymbol{\Theta})$, and $\mathbf{Q}$ denote the mass matrix, velocity coupling vector, gravity vector, and generalized force vector, respectively. Whereas $\ddot{\boldsymbol{\Theta}} = [\mathbf{a}^{\mathsf{T}},\ \boldsymbol{\alpha}^{\mathsf{T}},\ \ddot{\boldsymbol{\theta}}_{\mathbf{1}}^{\mathsf{T}},\ \ddot{\boldsymbol{\theta}}_{\mathbf{2}}^{\mathsf{T}}]^{\mathsf{T}}$ is the vector of accelerations, where $\mathbf{a} = [\ddot{x},\ \ddot{y},\ \ddot{z}]^{\mathsf{T}}$ is the linear acceleration vector of the pelvis, $\boldsymbol{\alpha} = [\ddot{\phi},\ \ddot{\varphi},\ \ddot{\psi}]^{\mathsf{T}}$ is the angular acceleration vector of the pelvis, and $\ddot{\boldsymbol{\theta}}_{\boldsymbol{k}} = [\ddot{\theta}_{k_1},\ \ddot{\theta}_{k_2},\ \ddot{\theta}_{k_3},\ \ddot{\theta}_{k_4}]^{\mathsf{T}}$ are joint acceleration vectors of the actuated joints in the lower limbs. The dynamic analysis may be divided in four parts – ground reaction forces, lower limbs, upper body, and pelvis. The interaction between main body and branches is considered in the following subsections.

3.3 Ground Reaction Forces

Force plates are a common instrument used in gait laboratories to measure ground reaction forces (GRF), but have the inconvenience of being fixed to the floor. Wearable force plates have been implemented under the shoe sole [20], which allow patients to walk outside laboratories and are

an excellent alternative for gait analysis. Nevertheless, the cost of having these devices attached permanently to the passive ankle-foot orthosis would make them less attractive. As an alternative, inexpensive pressure insoles can be used to estimate the GRF. Pressure insoles only provide the vertical component of the GRF, to determine the shear components Forner Cordero *et al.* [21] proposed to combine the insole measurement with the analytical representation of the GRF, i.e.,

$$\mathbf{F}_{_{TR}} = \sum_{i=1}^{n} m_i(\ddot{\mathbf{x}}_i + \mathbf{g}) \tag{3}$$

$$\mathbf{M}_{_{TR}} = \sum_{i=1}^{n} \frac{d(\mathbf{I}_i\, \boldsymbol{\omega}_i)}{dt} = \sum_{i=1}^{n} \mathbf{I}_i\, \boldsymbol{\alpha}_i + \boldsymbol{\omega}_i \times \mathbf{I}_i\, \boldsymbol{\omega}_i \tag{4}$$

where $\mathbf{F}_{_{TR}}$ is the total reaction force, m_i is the mass of the i^{th} body segment, $\ddot{\mathbf{x}}_i$ is the acceleration of the centre of mass, $\mathbf{g}$ is the gravity vector, $\mathbf{M}_{_{TR}}$ is the total reaction moment, $\mathbf{I}_i$ is the tensor of inertia, $\boldsymbol{\alpha}_i$ is the angular acceleration, and $\boldsymbol{\omega}_i$ is the angular velocity. The accelerations and velocities of the segments can be obtained with inertial sensors for a real application or with the inverse dynamics for a simulation. The GRF for each foot can be determined by decomposing $\mathbf{F}_{_{TR}}$ based on the location of the total centre of pressure obtained from the pressure insoles [21].

3.4 Dynamic Analysis of Lower Limbs

The Newton-Euler double-recursive formulation is a commonly used algorithm for finding the dynamic equation of robot manipulators. The closed-form dynamic equation can be used for both inverse and forward dynamic problems. The formulation consists of two iterations – outward and inward. In the outward iteration velocities and accelerations are evaluated and are used to determine the inertial force and the inertial moment acting at the centre of mass of the body segment. The iteration begins from the first link frame and moves successively to the last link, as the velocities and accelerations propagate in an outward fashion.

Outward Iterations: $i : Pv \rightarrow 3$

$$\begin{aligned}
{}^{i+1}\boldsymbol{\omega}_{i+1} &= {}^{i+1}_{i}\mathbf{R}\, {}^{i}\boldsymbol{\omega}_i + \dot{\theta}_{i+1}\, {}^{i+1}\hat{\mathbf{z}}_{i+1} \\
{}^{i+1}\dot{\boldsymbol{\omega}}_{i+1} &= {}^{i+1}_{i}\mathbf{R}\, {}^{i}\dot{\boldsymbol{\omega}}_i + {}^{i+1}_{i}\mathbf{R}\, {}^{i}\boldsymbol{\omega}_i \times \dot{\theta}_{i+1}\, {}^{i+1}\hat{\mathbf{z}}_{i+1} + \ddot{\theta}_{i+1}\, {}^{i+1}\hat{\mathbf{z}}_{i+1} \\
{}^{i+1}\dot{\mathbf{v}}_{i+1} &= {}^{i+1}_{i}\mathbf{R}\, ({}^{i}\dot{\boldsymbol{\omega}}_i \times {}^{i}\mathbf{P}_{i+1} + {}^{i}\boldsymbol{\omega}_i \times ({}^{i}\boldsymbol{\omega}_i \times {}^{i}\mathbf{P}_{i+1}) + {}^{i}\dot{\mathbf{v}}_i) \\
{}^{i+1}\dot{\mathbf{v}}_{c_{i+1}} &= {}^{i+1}\dot{\boldsymbol{\omega}}_{i+1} \times {}^{i+1}\mathbf{P}_{c_{i+1}} + {}^{i+1}\boldsymbol{\omega}_{i+1} \times ({}^{i+1}\boldsymbol{\omega}_{i+1} \times {}^{i+1}\mathbf{P}_{c_{i+1}}) \\
&\quad + {}^{i+1}\dot{\mathbf{v}}_{i+1} \\
{}^{i+1}\mathbf{F}_{i+1} &= m_{i+1}\, {}^{i+1}\dot{\mathbf{v}}_{c_{i+1}} \\
{}^{i+1}\mathbf{N}_{i+1} &= {}^{c_{i+1}}\mathbf{I}_{i+1}\, {}^{i+1}\dot{\boldsymbol{\omega}}_{i+1} + {}^{i+1}\boldsymbol{\omega}_{i+1} \times {}^{c_{i+1}}\mathbf{I}_{i+1}\, {}^{i+1}\boldsymbol{\omega}_{i+1}
\end{aligned}$$

Since the base reference frame is located at the pelvis, which moves freely with the body, it is necessary to establish some initial conditions. The angular velocity, angular acceleration, and linear acceleration of the pelvis along with the gravity vector are entered in the iteration as ${}^{Pv}\boldsymbol{\omega}_{_{Pv}} = [\dot{\phi},\ \dot{\varphi},\ \dot{\psi}]^{\intercal}$, ${}^{Pv}\dot{\boldsymbol{\omega}}_{_{Pv}} = [\ddot{\phi},\ \ddot{\varphi},\ \ddot{\psi}]^{\intercal}$, and ${}^{Pv}\dot{\mathbf{v}}_{_{Pv}} = [\ddot{x} + g_x,\ \ \ddot{y} + g_y,\ \ \ddot{z} + g_z]^{\intercal}$, respectively. The first iteration $(i : Pv \rightarrow 0)$ does not involve any joint displacement, i.e., $\dot{\theta}_0 = \ddot{\theta}_0 = 0$.

No rigid links exist within joint centres at the hip joint; therefore, $m_0 = m_1 = m_2 = 0$, ${}^0\mathbf{P}_{c_0} = {}^1\mathbf{P}_{c_1} = {}^2\mathbf{P}_{c_2} = \mathbf{0}$, and ${}^{c_0}\mathbf{I}_0 = {}^{c_1}\mathbf{I}_1 = {}^{c_2}\mathbf{I}_2 = \mathbf{0}$. Iterations 3 and 4 describe the thigh and shank segments, whose parameters are given in Table 2. Note, the parameters regarding the exoskeleton have not been considered as its design has not been developed yet. However, the mass and inertia properties of the exoskeleton must be added to the formulation.

In the inward iteration, the reaction forces and moments acting at the joints are derived. The iteration, which involves force and moment balance equations, starts at the last link and moves sequentially inward toward the first link frame.

Inward Iterations: $i : 4 \rightarrow 0$ (as Pv is the base frame)

$$
\begin{aligned}
{}^i\mathbf{f}_i &= {}^i_{i+1}\mathbf{R}\,{}^{i+1}\mathbf{f}_{i+1} + {}^i\mathbf{F}_i \\
{}^i n_i &= {}^i\mathbf{N}_i + {}^i_{i+1}\mathbf{R}\,{}^{i+1}\mathbf{n}_{i+1} + {}^i\mathbf{P}_{c_i} \times {}^i\mathbf{F}_i + {}^i\mathbf{P}_{i+1} \times {}^i_{i+1}\mathbf{R}\,{}^{i+1}\mathbf{f}_{i+1} \\
\tau_i &= {}^i\mathbf{n}_i^T\,{}^i\hat{\mathbf{z}}_i
\end{aligned}
$$

where ${}^5\mathbf{f}_5$ and ${}^5\mathbf{n}_5$ represent the external forces acting at the ankle joint. These are obtained with a free-body-diagram of the foot including the GRF derived in the previous section.

The following dynamic equation results,

$$
\mathbf{M}_{\theta_k/a}(\boldsymbol{\theta_k})\mathbf{a} + \mathbf{M}_{\theta_k/\alpha}(\boldsymbol{\theta_k})\boldsymbol{\alpha} + \mathbf{M}_{\theta_k}(\boldsymbol{\theta_k})\ddot{\boldsymbol{\theta}}_{\boldsymbol{k}} + \mathbf{V}_{\theta_k}(\boldsymbol{\omega}, \dot{\boldsymbol{\theta}}_{\boldsymbol{k}}, \boldsymbol{\theta_k}) + \boldsymbol{G}_{\theta_k}(\boldsymbol{\theta_k}) = \mathbf{Q_k} \tag{5}
$$

where $\mathbf{Q_k} = \boldsymbol{\tau}_{\theta_k} - \mathbf{J}^{\mathsf{T}}_{\theta_k}\mathbf{F}_{\theta_k}$, with $\boldsymbol{\tau}_{\theta_k}$ and $\mathbf{F}_{\theta_k}$ being joint torques and external forces/moments.

3.5 Dynamic Analysis of Upper Body

Forces and moments acting on the upper body, due to gravity, inertia, or external forces, play an important role on the dynamics and balance of the whole system. The objective of this section is to determine the reaction forces and moments of the upper body on the pelvis. This reaction is expressed numerically with the information gathered from inertial sensors in a real application, or with the inverse dynamics analysis in a computer simulation. The motion of the upper body is subject to the motion of the pelvis plus the contribution in motion of each individual degree of freedom contained in the upper body. For the computer simulation, the Newton-Euler recursive formulation is used to determine the reaction forces and moments at the shoulders and neck. The reactions at the sacroiliac joint are determined using Newton and Euler equations of motion.

$$
\mathbf{f}_{_S} = m_{_{TA}}\,(\mathbf{a}_{_{TA}} - \mathbf{g}) - \sum \mathbf{f}_{_{UB}} \tag{6}
$$

$$
\mathbf{n}_{_S} = \mathbf{I}_{_{TA}}\,\boldsymbol{\alpha}_{_{TA}} + \boldsymbol{\omega}_{_{TA}} \times \mathbf{I}_{_{TA}}\,\boldsymbol{\omega}_{_{TA}} + \mathbf{r}_{c_{TA}} \times m_{_{TA}}\,(\mathbf{a}_{_{TA}} - \mathbf{g}) - \sum \mathbf{n}_{_{UB}} - \sum \mathbf{r}_{_{UB}} \times \mathbf{f}_{_{UB}} \tag{7}
$$

where subscript ${}_{_{TA}}$ denotes the thorax-abdomen segment, $\sum \mathbf{f}_{_{UB}}$ and $\sum \mathbf{n}_{_{UB}}$ indicate the sum of other reaction forces and moments (shoulders and neck), and $\mathbf{r}$ is the moment arm.

3.6 Dynamic Analysis of the Pelvis

The pelvis is subject to the reaction forces and moments acting at the hip and sacroiliac joints. Applying Newton's second law yields

$$
\sum \mathbf{f} = \mathbf{f}_{_{H_1}} + \mathbf{f}_{_{H_2}} + \mathbf{f}_{_S} + m_{_{Pv}}\mathbf{g} = m_{_{Pv}}\mathbf{a}_{_{Pv}}. \tag{8}
$$

The reaction forces at the hips can be determined by transforming the reaction force from frame {0} to frame {Pv}, which was previously found in the inward iteration, i.e., $\mathbf{f}_{H_k} = -\,{}^{Pv}_{0}\mathbf{R}\;{}^{0}\mathbf{f}_0$, where ${}^{Pv}_{0}\mathbf{R}$ happens to be an identity matrix and the negative sign is to convert the net forces applied to the link (as set-up in the inward iteration) with the reaction forces acting at the hip. After expanding and grouping similar terms, the following expression results

$$\mathbf{f}_{H_k} = -(\mathbf{M}_{f/a}(\boldsymbol{\theta_k})\mathbf{a} \;+\; \mathbf{M}_{f/\alpha}(\boldsymbol{\theta_k})\boldsymbol{\alpha} \;+\; \mathbf{M}_{f/\theta_k}(\boldsymbol{\theta_k})\ddot{\boldsymbol{\theta}}_{\boldsymbol{k}} \;+\; \mathbf{V}_f(\boldsymbol{\omega}, \dot{\boldsymbol{\theta}}_{\boldsymbol{k}}, \boldsymbol{\theta_k}) \;+\; \mathbf{G}_f(\boldsymbol{\theta_k})) \tag{9}$$

By combining Eqs. (8 - 9), the following equation of motion yields

$$\begin{aligned}&(\mathbf{M}_{Pv} \;+\; \mathbf{M}_{f/a}(\boldsymbol{\theta_1}) \;+\; \mathbf{M}_{f/a}(\boldsymbol{\theta_2}))\mathbf{a} \;+\; (\mathbf{M}_{f/\alpha}(\boldsymbol{\theta_1}) \;+\; \mathbf{M}_{f/\alpha}(\boldsymbol{\theta_2}))\boldsymbol{\alpha} \;+\mathbf{M}_{f/\theta_1}(\boldsymbol{\theta_1})\ddot{\boldsymbol{\theta}}_{\mathbf{1}} + \\ &\mathbf{M}_{f/\theta_2}(\boldsymbol{\theta_2})\ddot{\boldsymbol{\theta}}_{\mathbf{2}} \;+\mathbf{V}_f(\boldsymbol{\omega}, \dot{\boldsymbol{\theta}}_{\mathbf{1}}, \boldsymbol{\theta_1}) \;+\; \mathbf{V}_f(\boldsymbol{\omega}, \dot{\boldsymbol{\theta}}_{\mathbf{2}}, \boldsymbol{\theta_2}) \;+\mathbf{G}_f(\boldsymbol{\theta_1}) \;+\; \mathbf{G}_f(\boldsymbol{\theta_2}) \;=\; \mathbf{F}_f\end{aligned} \tag{10}$$

where $\mathbf{M}_{Pv}$ is a diagonal matrix that contains the mass of the pelvis and $\mathbf{F}_f = \mathbf{f}_S + m_{Pv}\mathbf{g}$.

The moment analysis is carried out with Euler's equation of motion, i.e,

$$\sum \mathbf{n}_{Pv} = \mathbf{n}_{H_1} + \mathbf{n}_{H_2} + \mathbf{n}_S + \mathbf{r}_S \times \mathbf{f}_S = \mathbf{I}_{Pv}\,\boldsymbol{\alpha}_{Pv} + \boldsymbol{\omega}_{Pv} \times \mathbf{I}_{Pv}\,\boldsymbol{\omega}_{Pv}. \tag{11}$$

The contribution to the net moment by the legs is obtained with $\mathbf{n}_{H_k} = -({}^{Pv}_{0}\mathbf{R}\;{}^{0}\mathbf{n}_0 \;+\; {}^{Pv}\mathbf{P}_0 \;\times\; {}^{Pv}_{0}\mathbf{R}\;{}^{0}\mathbf{f}_0)$. After expanding and grouping similar terms, the following expression results,

$$\mathbf{n}_{H_k} \;=\; -(\mathbf{M}_{n/a}(\boldsymbol{\theta_k})\mathbf{a} \;+\; \mathbf{M}_{n/\alpha}(\boldsymbol{\theta_k})\boldsymbol{\alpha} \;+\; \mathbf{M}_{n/\theta_k}(\boldsymbol{\theta_k})\ddot{\boldsymbol{\theta}}_{\boldsymbol{k}} \;+\; \mathbf{V}_n(\boldsymbol{\omega}, \dot{\boldsymbol{\theta}}_{\boldsymbol{k}}, \boldsymbol{\theta_k}) \;+\; \mathbf{G}_n(\boldsymbol{\theta_k})). \tag{12}$$

By combining Eqs. (11 - 12), the following equation of motion results

$$\begin{aligned}&(\mathbf{M}_{n/a}(\boldsymbol{\theta_1}) \;+\; \mathbf{M}_{n/a}(\boldsymbol{\theta_2}))\mathbf{a} \;+\; (\mathbf{I}_{Pv} \;+\; \mathbf{M}_{n/\alpha}(\boldsymbol{\theta_1}) \;+\; \mathbf{M}_{n/\alpha}(\boldsymbol{\theta_2}))\boldsymbol{\alpha} \;+\mathbf{M}_{n/\theta_1}(\boldsymbol{\theta_1})\ddot{\boldsymbol{\theta}}_{\mathbf{1}} + \\ &\mathbf{M}_{n/\theta_2}(\boldsymbol{\theta_2})\ddot{\boldsymbol{\theta}}_{\mathbf{2}} \;+\; \mathbf{V}_n(\boldsymbol{\omega}, \dot{\boldsymbol{\theta}}_{\mathbf{1}}, \boldsymbol{\theta_1}) \;+\; \mathbf{V}_n(\boldsymbol{\omega}, \dot{\boldsymbol{\theta}}_{\mathbf{2}}, \boldsymbol{\theta_2}) \;+\; \mathbf{G}_n(\boldsymbol{\theta_1}) \;+\; \mathbf{G}_n(\boldsymbol{\theta_2}) \;=\; \mathbf{n}_f\end{aligned} \tag{13}$$

where $\mathbf{n}_f \;=\; \mathbf{n}_S + \mathbf{r}_S \times \mathbf{f}_S$

3.7 Closed-Form Dynamics

The equations of motion of the lower limbs and pelvis are combined into one equation that represents the equation of motion of the overall system, i.e.,

$$\mathbf{M}(\boldsymbol{\theta_1}, \boldsymbol{\theta_2}) \begin{bmatrix} \mathbf{a} \\ \boldsymbol{\alpha} \\ \ddot{\boldsymbol{\theta}}_{\mathbf{1}} \\ \ddot{\boldsymbol{\theta}}_{\mathbf{2}} \end{bmatrix} + \begin{bmatrix} \mathbf{V}_f(\boldsymbol{\omega}, \dot{\boldsymbol{\theta}}_{\boldsymbol{k}}, \boldsymbol{\theta_k}) \\ \mathbf{V}_n(\boldsymbol{\omega}, \dot{\boldsymbol{\theta}}_{\boldsymbol{k}}, \boldsymbol{\theta_k}) \\ \mathbf{V}_{\theta_1}(\boldsymbol{\omega}, \dot{\boldsymbol{\theta}}_{\mathbf{1}}, \boldsymbol{\theta_1}) \\ \mathbf{V}_{\theta_2}(\boldsymbol{\omega}, \dot{\boldsymbol{\theta}}_{\mathbf{2}}, \boldsymbol{\theta_2}) \end{bmatrix} + \begin{bmatrix} \mathbf{G}_f(\boldsymbol{\theta_k}) \\ \mathbf{G}_n(\boldsymbol{\theta_k}) \\ \boldsymbol{G}_{\theta_1}(\boldsymbol{\theta_1}) \\ \boldsymbol{G}_{\theta_2}(\boldsymbol{\theta_2}) \end{bmatrix} = \begin{bmatrix} \mathbf{0} \\ \mathbf{0} \\ \boldsymbol{\tau}_{\theta_1} \\ \boldsymbol{\tau}_{\theta_2} \end{bmatrix} - \begin{bmatrix} \mathbf{F}_f \\ \mathbf{n}_f \\ \mathbf{J}^{\intercal}_{\theta_1}\,\mathbf{F}_{\theta_1} \\ \mathbf{J}^{\intercal}_{\theta_2}\,\mathbf{F}_{\theta_2} \end{bmatrix} \tag{14}$$

where $\mathbf{M}(\boldsymbol{\theta_1}, \boldsymbol{\theta_2})$ is a symmetric positive definite of the form

$$\mathbf{M}(\boldsymbol{\theta_1}, \boldsymbol{\theta_2}) \;=\; \begin{bmatrix} \mathbf{M}_{f/a}(\boldsymbol{\theta_1}, \boldsymbol{\theta_2}) & \mathbf{M}_{f/\alpha}(\boldsymbol{\theta_1}, \boldsymbol{\theta_2}) & \mathbf{M}_{f/\theta_1}(\boldsymbol{\theta_1}) & \mathbf{M}_{f/\theta_2}(\boldsymbol{\theta_2}) \\ \mathbf{M}_{n/a}(\boldsymbol{\theta_1}, \boldsymbol{\theta_2}) & \mathbf{M}_{n/\alpha}(\boldsymbol{\theta_1}, \boldsymbol{\theta_2}) & \mathbf{M}_{n/\theta_1}(\boldsymbol{\theta_1}) & \mathbf{M}_{n/\theta_2}(\boldsymbol{\theta_2}) \\ \mathbf{M}_{\theta_1/a}(\boldsymbol{\theta_1}) & \mathbf{M}_{\theta_1/\alpha}(\boldsymbol{\theta_1}) & \mathbf{M}_{\theta_1}(\boldsymbol{\theta_1}) & \mathbf{0} \\ \mathbf{M}_{\theta_2/a}(\boldsymbol{\theta_2}) & \mathbf{M}_{\theta_2/\alpha}(\boldsymbol{\theta_2}) & \mathbf{0} & \mathbf{M}_{\theta_2}(\boldsymbol{\theta_2}) \end{bmatrix}$$

with $\mathbf{M}_{f/a}(\boldsymbol{\theta_1}, \boldsymbol{\theta_2}) \;=\; \mathbf{M}_T \;+\; \mathbf{M}_{f/a}(\boldsymbol{\theta_1}) + \mathbf{M}_{f/a}(\boldsymbol{\theta_2})$, $\mathbf{M}_{f/\alpha}(\boldsymbol{\theta_1}, \boldsymbol{\theta_2}) \;=\; \mathbf{M}_{f/\alpha}(\boldsymbol{\theta_1}) + \mathbf{M}_{f/\alpha}(\boldsymbol{\theta_2})$, $\mathbf{M}_{n/a}(\boldsymbol{\theta_1}, \boldsymbol{\theta_2}) = \mathbf{M}_{n/a}(\boldsymbol{\theta_1}) \;+\; \mathbf{M}_{n/a}(\boldsymbol{\theta_2})$, and $\mathbf{M}_{n/\alpha}(\boldsymbol{\theta_1}, \boldsymbol{\theta_2}) = \mathbf{I}_T \;+\; \mathbf{M}_{n/\alpha}(\boldsymbol{\theta_1}) \;+\; \mathbf{M}_{n/\alpha}(\boldsymbol{\theta_2})$.

4 FUTURE WORK

This work is the beginning of a very ambitious project. Currently, a trajectory generator is being developed for a complete human gait cycle. Data gathered from testing an individual wearing inertial/magnetic sensors will be used. Correlation between the trajectory and the contact with the floor will be analyzed. A simulation of the dynamic model will be performed and different control strategies that follow the generated trajectory will be tested. Collision detection will be implemented in the simulation. The different types of contact that a person may experience on a dynamic environment – no external contact, rigid contact, soft contact, and instantaneous impact – will be studied. Conventional indices of balance – CoM, ZMP, FRI – will be incorporated and 'an optimal' trajectory will be developed. Eventually, bio-electrical sensors will used to predict the intended motion of the user and a learning controller that is able to optimize online human gait trajectories will be developed.

5 CONCLUSIONS

Human-body kinematic and dynamic models for paraplegics wearing an ambulatory exoskeleton were developed. The whole body was modelled with 34-dof – torso (3-dof), neck (3-dof), legs (2×7-dof), and arms (2×7-dof). The dynamic model represents the human body as a free spatial system that performs different actions by interacting with the exterior through contact forces. There are fourteen state variables in the dynamic model – the six coordinates that describe the main body (pelvis) in space and the eight joint displacements of the exoskeleton's actuators. The effect of the ground reaction forces on the exoskeleton and a potential implementation based on inexpensive pressure insoles were investigated. A 3D model of a human body represented by fifteen segments was developed in Matlab. Anthropomorphic parameters were assigned to each segment.

REFERENCES

[1] General Electric Co., "Hardiman I Prototype Project, Special Interim Study", General Electric Report S6-68-1060, Schenectady, NY, 1968.

[2] Kazerooni, H., Steger, R., and Huang, L., "Hybrid Control of the Berkeley Lower Extremity Exoskeleton (BLEEX)," *International Journal of Robotics Research*, 25(5-6), pp. 561-573, May-June 2006.

[3] Jacobsen S.C., Olivier M., Smith F.M., Knutti D.F., Johnson R.T., Colvin G.E., and Scroggin W.B., "Research Robots for Applications in Artificial Intelligence, Teleoperation and Entertainment," *The International Journal of Robotics Research*, 23(4-5) , pp. 319-330, 2004.

[4] Sankai, Y., "Leading Edge of Cybernics: Robot Suit HAL," *International Joint Conference SICE-ICCAS 2006*, Busan (Korea), pp. 27-28, October 18-21, 2006.

[5] Vukobratovic M., Hristic D., and Stojiljkovic Z., "Development of Active Anthropomorphic Exoskeletons," *Medical and Biological Engineering*, 12(1), pp. 66-80, 1974.

[6] Seireg A. and Grundmann J. G., "Design of a Multitask Exoskeletal Walking Device for Paraplegics," *Biomechanics of Medical Devices*, NY: Marcel Dekker, pp. 569-644, 1981.

[7] Kong K. and Jeon D.,"Design and Control of an Exoskeleton for the Elderly and Patients," *IEEE/ASME Transactions on Mechatronics*, 11(4), pp. 428-432, 2006.

[8] Baker, B., "Walk of Life," *The Engineer*, 293(7750), pp. 30-31, June 16, 2008,

[9] Colombo G., Joerg M., Schreier R., and Dietz V., "Treadmill Training of Paraplegic Patients Using a Robotic Orthosis," *Journal of Rehabilitation Research and Development,* 37(6), pp. 693-700, 2000.

[10] Veneman, J. F., Ekkelenkamp, R., Kruidhof, R., van der Helm, F.C.T., and van der Kooij, H., "A Series Elastic- and Bowden-Cable-Based Actuation System for Use as Torque Actuator in Exoskeleton-Type Robots," *The International Journal of Robotics Research*, 25(3), pp. 261-281, 2006.

[11] Ferris D.P., Sawicki G.S., Domingo A., "Powered Lower Limb Orthoses for Gait Rehabilitation," *Topics in Spinal Cord Injury Rehabilitation,* 11(2), pp. 34-49, 2005.

[12] Zatsiorsky V. M., Kinematics of Human Motion. *Human Kinetics*, 1998.

[13] Pons, J. (ed.), Wearable Robots: Biomechatronic Exoskeletons. *Wiley*, 2008

[14] Mayol W., Tordoff B., and Murray D., "Designing a miniature wearable visual robot," *in Proceedings of the IEEE International Conference on Robotics and Automation* pp. 3725-3730, 2002.

[15] Dempster, W. T. and Gaughran, G. R. L., "Properties of Body Segments Based on Size and Weight," *American Journal of Anatomy*, 120(1), pp.33-54, 1967.

[16] Hanavan, E. P., "A Mathematical Model of the Human Body," *Technical Report,* Aerospace Medical Research Lab., Wright-Patterson Air Force Base, OH., 158 pages, 1964.

[17] Zatsiorsky, V. M., Seluyanov, V. N. and Chugunova, L. G., "Methods of determining mass-inertial characteristics of human body segments," *In Contemporary Problems of Biomechanics*, (Ed. Chemyi G. G. and Regirer, S. A.), CRC Press, MA, pp. 272-291, 1990.

[18] De Leva, P., "Adjustments to Zatsiorsky-Seluyanov's segment inertia parameters," *Journal of Biomechanics*, 29(9), pp. 1223-1230, 1996.

[19] Vukobratović, M., Potkonjak, V., Babković, K. and Borovac, B. "Simulation Model of General Human and Humanoid Motion," *Multibody System Dynamics*, 17(1), pp. 71-96, 2007.

[20] Chao L.-P and Yin C.-Y. "The Six-Component Force Sensor for Measuring the Loading of the Feet in Locomotion," *Materials and Design*, 20(5), pp. 237-244, 1999.

[21] Forner-Cordero A., Koopman H., and van der Helm F., "Use of Pressure Insoles to Calculate the Complete Ground Reaction Forces," *Journal of Biomechanics,* 37, pp. 1427-32, 2004.